ceramics

MDPI

Article

Structural and Mechanical Properties of Amorphous Si_3N_4 Nanoparticles Reinforced Al Matrix Composites Prepared by Microwave Sintering

Manohar Reddy Mattli [1], Penchal Reddy Matli [2], Abdul Shakoor [1,*] and Adel Mohamed Amer Mohamed [3]

[1] Center for Advanced Materials, Qatar University, Doha 2713, Qatar; manoharreddy892@gmail.com
[2] Department of Mechanical Engineering, National University of Singapore, Singapore 117576, Singapore; drlpenchal@nus.edu.sg
[3] Department of Metallurgical and Materials Engineering, Faculty of Petroleum and Mining Engineering, Suez University, Suez 43721, Egypt; adel.mohamed25@yahoo.com
* Correspondence: shakoor@qu.edu.qa; Tel.: +974-44036867

Received: 10 January 2019; Accepted: 13 February 2019; Published: 14 February 2019

Abstract: The present study focuses on the synthesis and characterization of amorphous silicon nitride (Si_3N_4) reinforced aluminum matrix nanocomposites through the microwave sintering process. The effect of Si_3N_4 (0, 1, 2 and 3 wt.%) nanoparticles addition to the microstructure and mechanical properties of the Al-Si_3N_4 nanocomposites were investigated. The density of Al-Si_3N_4 nanocomposites increased with increased Si_3N_4 content, while porosity decreased. X-ray diffraction (XRD) analysis reveals the presence of Si_3N_4 nanoparticles in Al matrix. Microstructural investigation of the nanocomposites shows the uniform distribution of Si_3N_4 nanoparticles in the aluminum matrix. Mechanical properties of the composites were found to increase with an increasing volume fraction of amorphous Si_3N_4 reinforcement particles. Al-Si_3N_4 nanocomposites exhibits higher hardness, yield strength and enhanced compressive performance than the pure Al matrix. A maximum increase of approximately 72% and 37% in ultimate compressive strength and 0.2% yield strength are achieved. Among the synthesized nanocomposites, Al-3wt.% Si_3N_4 nanocomposites displayed the maximum hardness (77 $\pm$ 2 Hv) and compressive strength (364 $\pm$ 2 MPa) with minimum porosity level of 1.1%.

Keywords: aluminum; amorphous silicon nitride; microwave sintering; microstructural; mechanical properties

1. Introduction

Aluminum metal matrix composites (AMMCs) have been widely used and have vast applications in automotive and aerospace industries due to their light weight, low density, high strength to weight ratio and attractive properties [1–3]. The process of choosing the matrix and reinforcement is complex, and by adding suitable reinforcements to the matrix material, the properties of the composites can be tailored to meet the specific requirements. The main aim to develop the aluminum metal matrix composites is to produce materials that are lightweight, high strength, and lower cost when compared to the aluminum and traditional aluminum alloys.

Aluminum is the most commonly used matrix material in metal matrix composites. Ceramics that are generally used as the reinforcements in metal matrix composites are SiC, B_4C, Si_3N_4, Al_2O_3, Y_2O_3, and TiC. These reinforcements provide better microstructure and mechanical properties when combined with the metal matrix materials [4]. When compared to monolithic aluminum, Al-based metal matrix composites shows the significant improvement in mechanical properties in terms of

enhanced strength and stiffness, good fatigue and wear resistance, less weight and high-temperature stability [5–8].

There are different methods available to fabricate the aluminum metal matrix composites, such as powder metallurgy, forging and stir casting routs [9–11]. Among these, powder metallurgy (PM) technique, involving blending, compaction and sintering, is one of the common methods used in the synthesis of metal matrix composites. In the blending process, planetary ball mill was used for blending the matrix and reinforcements powders in order to get uniform distribution of nanoparticles in the matrix phase. The sintering process has the ability to develop the microstructural and mechanical properties of the final synthesized product. There are many heating processes in the sintering method, such as microwave, vacuum, spark plasma, and the conventional sintering process [12–14]. In the microwave sintering process, heat is generated within the samples by rapid oscillation of dipoles at microwave frequencies. Additionally, uniform volumetric heating of the microwave sintering results in significant improvement in the microstructure and mechanical properties.

So far, few ceramic materials are used as the reinforcing materials like SiC, B_4C, Si_3N_4, Al_2O_3, Y_2O_3, TiC and TiB_2, and so on, in metal matrix composites [15–18]. Among these ceramic reinforcements, amorphous silicon nitride (Si_3N_4) is selected as the reinforcement used in the present study owing to its good mechanical, thermal and electrical properties, superior corrosion and good thermal stability [19–21]. To the best of authors knowledge, there has been no study conducted on the compressive behavior of the amorphous silicon nitride (Si_3N_4) reinforced Al-matrix nanocomposites.

The present research work deals with the fabrication and characterization of Al-Si_3N_4 nanocomposites using microwave sintering technique (MWS) and the effect of varying contents of amorphous Si_3N_4 nanoparticles on the microstructure and compressive performance of the synthesized nanocomposites were investigated in detail.

2. Materials and Methods

Pure Al (99.5% purity, ~10 µm, Alfa Aesar, Tewksbury, MA, USA) and amorphous Si_3N_4 nanoparticles (98.5+% purity, ~15–30 nm, Alfa Aesar, USA) were used as raw materials for the synthesis of Al-Si_3N_4 nanocomposites. Aluminum powder was mixed with 0, 1, 2 and 3wt.% of amorphous Si_3N_4 nanoparticles. The blending of two mixtures was carried out at room temperature in a planetary ball mill (PM 200) for 2 hours with the 200 rpm. No balls were used during the blending of powders. The blended powder was compacted into cylindrical pellets by applying uniaxial pressure of 50 MPa with holding time of 1 min. The compacted cylindrical pellets were sintered in a microwave sintering furnace at 550 °C with a heating rate of 10 °C/min for 30 min. The compacted pellets were placed at the center of the cavity and sintering was performed inside the multimode cavity [22]. The schematic of the experimental procedure is presented in Figure 1.

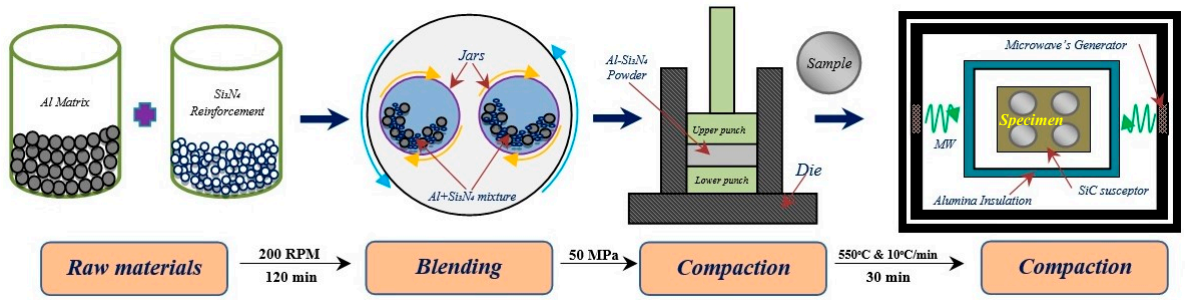

Figure 1. Schematic diagram of Si_3N_4 nanoparticle-reinforced Al nanocomposites.

The density of the microwave sintered samples was calculated by using the Archimedes' principle. The X-ray diffraction (XRD, PANalytical X'pert pro) analysis was performed to identify the phases present in Al-Si_3N_4 nanocomposites and to identify the presence of any impurities in the developed

composites. The XRD analysis was performed in the 2θ range of 30–90° with a scanning rate of 1.5°/min. The morphology of the sintered composites was observed using scanning electron microscopy (SEM, JeolNeoscope JSM6000, Peabody, MA, USA) equipped with energy dispersive X-ray spectroscopy (EDX).

The microhardness of the Al-Si_3N_4 nanocomposites was determined by using Vickers Microhardness tester (MKV-h21) with an applied load of 25 gf and a dwell time of 10 s, for each sample with an average of 5 successive indentations.

Compression analysis of the nanocomposites was performed at room temperature by using the universal testing machine (UTM-Lloyd), under an engineering strain rate of 10^{-4}/s. The respective data of each sample was obtained by an average of three successive values of test results. Yield strength (YS), ultimate compressive strength (UCS) and failure strain (FS) values of the nanocomposites were calculated by the obtained stress-strain curves. Fractographic analysis was performed to study the fractured surfaces of the Al-Si_3N_4 nanocomposites by using the field emission scanning electron microscope (Hitachi FESEM-S4300, Tokyo, Japan).

3. Experimental Analysis

3.1. Density and Porosity of Al-Si_3N_4 Nanocomposites

Figure 2 shows the variation of density and porosity of the microwave sintered Al-Si_3N_4 nanocomposites with varying Si_3N_4 content. It can be observed from Figure 2 that the density of the composites increased with the increasing amorphous Si_3N_4 content, due to the higher density of Si_3N_4 phase [23]. The higher density of the sintered nanocomposites influences the microstructural and mechanical properties of the synthesized Al composite materials. The porosity of the composites has shown a decreasing trend with the increasing amount of amorphous Si_3N_4 content. The nature of the reinforcement content and volumetric heating phenomenon is one of the main reasons for the low porosity.

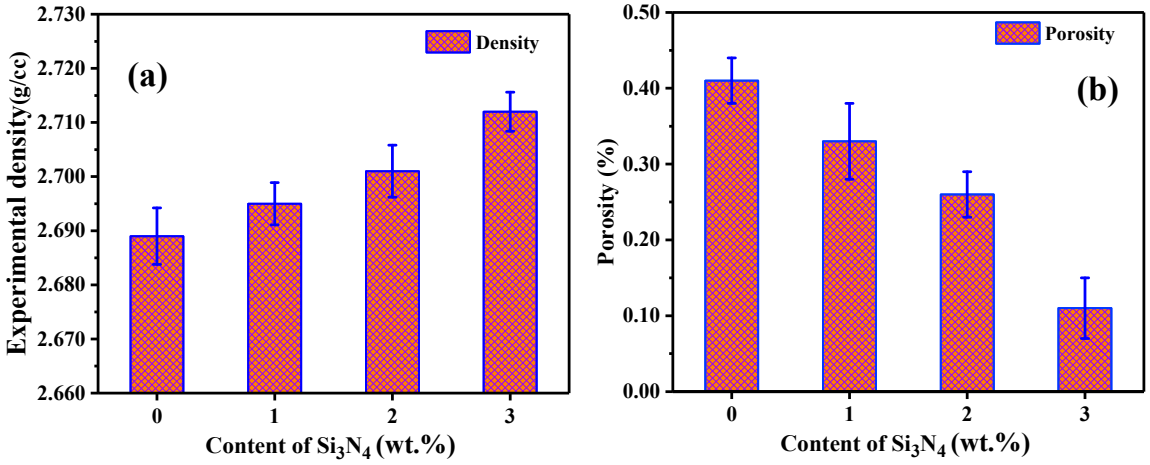

Figure 2. Variation of experimental density (**a**), and porosity (**b**) with Si_3N_4 content.

3.2. XRD Analysis of Al-Si_3N_4 Nanocomposites

Figure 3 shows the XRD patterns of the microwave sintered Al-Si_3N_4 nanocomposites. Figure 3b shows the enlarged pattern of the Al-3wt.% Si_3N_4 nanocomposite. The XRD patterns clearly indicate that the presence of Al and amorphous Si_3N_4 in Al-Si_3N_4 nanocomposites and also shows that no other phases and impurities are present in Al composites [24,25]. Due to the presence of a small percentage of the reinforcement content, the reinforcement phase appears smaller in intensity as compared to the peaks of the Al matrix phase. The intensity of the amorphous Si_3N_4 diffraction peak increased with the increasing amount of reinforcement content.

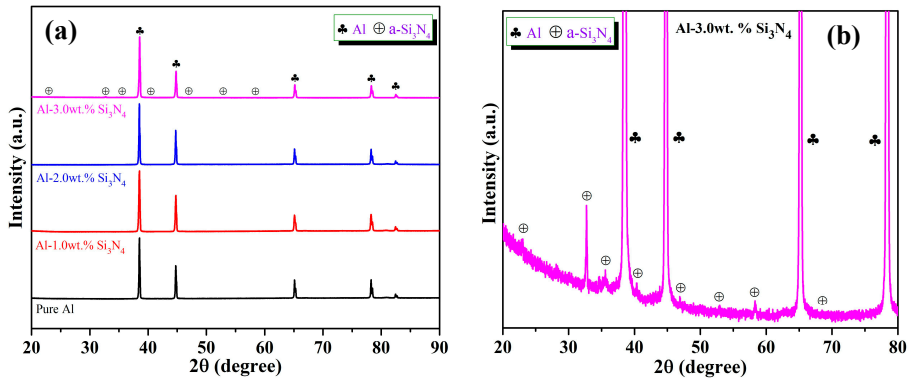

Figure 3. (**a**) X-ray diffraction (XRD) pattern of Al-Si_3N_4 nanocomposite, (**b**) Al-3wt.% of Si_3N_4 nanocomposites.

3.3. SEM Analysis of Al-Si_3N_4 Nanocomposites

Figure 4 shows SEM images of microwave sintered Al-Si_3N_4 nanocomposites with different Si_3N_4 contents. It can be observed that clearly the amorphous Si_3N_4 nanoparticles are homogeneously distributed in the Al matrix.

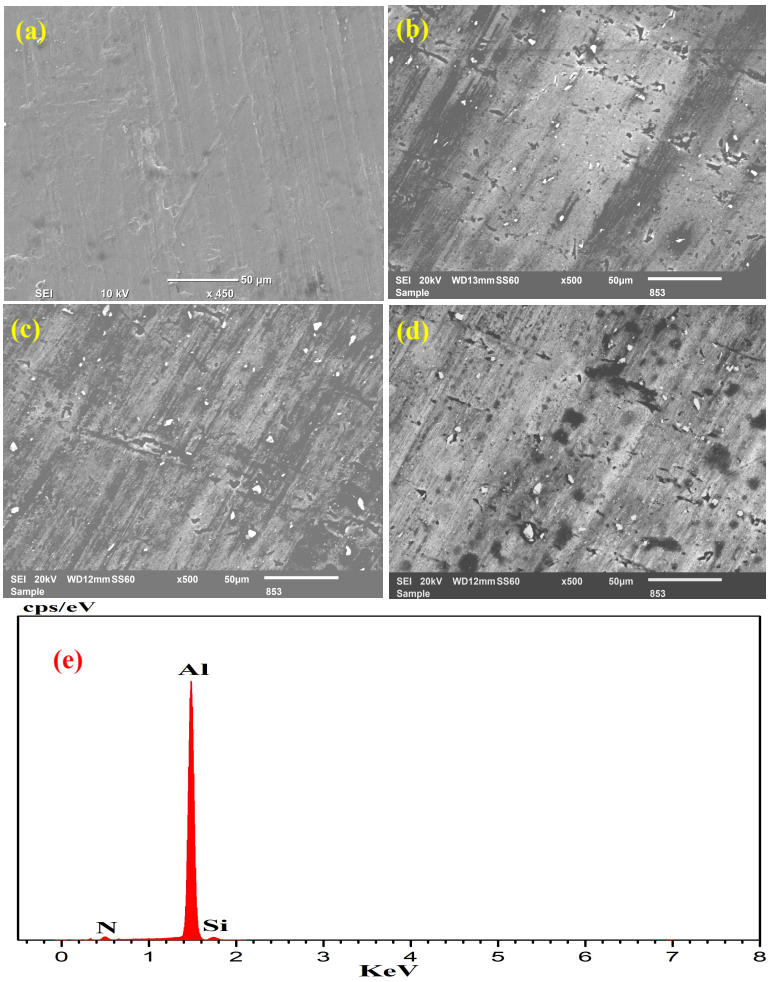

Figure 4. Scanning electron microscopy (SEM) images of the (**a**) pure Al (**b**) Al-1wt.% Si_3N_4 (**c**) Al-2wt.%Si_3N_4 (**d**) Al-3wt.% Si_3N_4 nanocomposites and (**e**) Energy dispersive X-ray spectroscopy (EDX) spectrum analysis of Al-2% Si_3N_4 nanocomposites.

The white color particles represent the amorphous silicon nitride and a gray phase represents the aluminum matrix. The EDS analysis was employed to identify the elemental distribution in the Al matrix. Figure 4e shows the EDX spectrum of Al-2wt.% Si_3N_4 nanocomposite was composed of mainly Al, Si and N elements. The homogeneous distribution and an excess amount of amorphous silicon nitride in aluminum matrix influence on the microstructure and mechanical properties of the Al- Si_3N_4 nanocomposites.

3.4. Microhardness of Al-Si_3N_4 Nanocomposites

Hardness is a useful mechanical property that provides valuable insight into the overall mechanical behaviour of composites. Generally, several factors would affect the microhardness of the composites such as particle size, amount of reinforcement and method of preparation. The effect of Si_3N_4 nanoparticles in Al composites is shown in Figure 5 and Table 1.

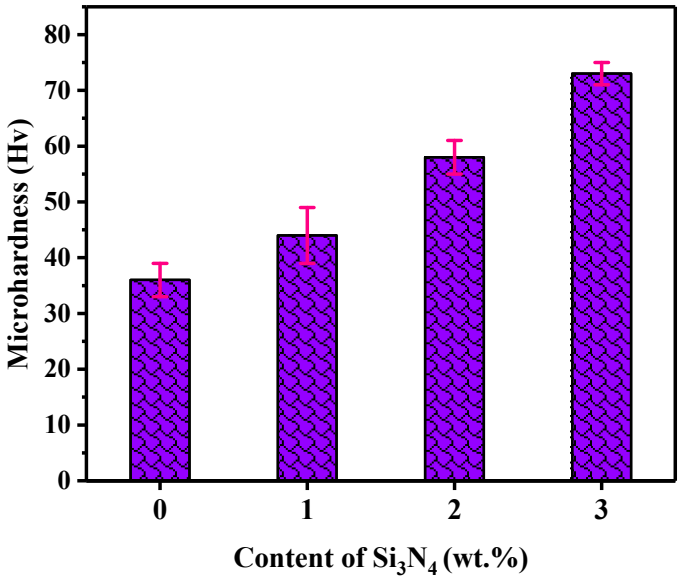

Figure 5. Microhardness of Al-Si_3N_4 nanocomposites versus Si_3N_4 content.

It can be clearly seen that the microhardness of the Al-Si_3N_4 nanocomposites gradually increased with the increase in amorphous Si_3N_4 content [26]. The Al-3wt.% Si_3N_4 composite has the highest hardness value (77 $\pm$ 4) when compared with that of pure Al. This higher value of the hardness of the nanocomposites can be associated with the presence of hard amorphous silicon nitride nanoparticles in the aluminum matrix and the dispersion hardening effect [27,28]. The microhardness of the microwave sintered samples in this study was found to be higher than the vacuum sintering samples [29].

The presence of hard amorphous Si_3N_4 nanoparticles improves the hardness of the composites materials as explained by the rule of mixtures [30].

$$H_c = H_m V_m + H_r V_r$$

where H_c represents the hardness of the composite, H_m and V_m represents the hardness and volume fraction of the matrix and H_r and V_r represents the hardness and volume fraction of the reinforcements, respectively.

3.5. Compressive Analysis of Al-Si_3N_4 Nanocomposites

Figure 6a presents the engineering stress-strain curves of the microwave sintered Al-Si_3N_4 nanocomposites and their corresponding mechanical data presented in Figure 6b and Table 1.

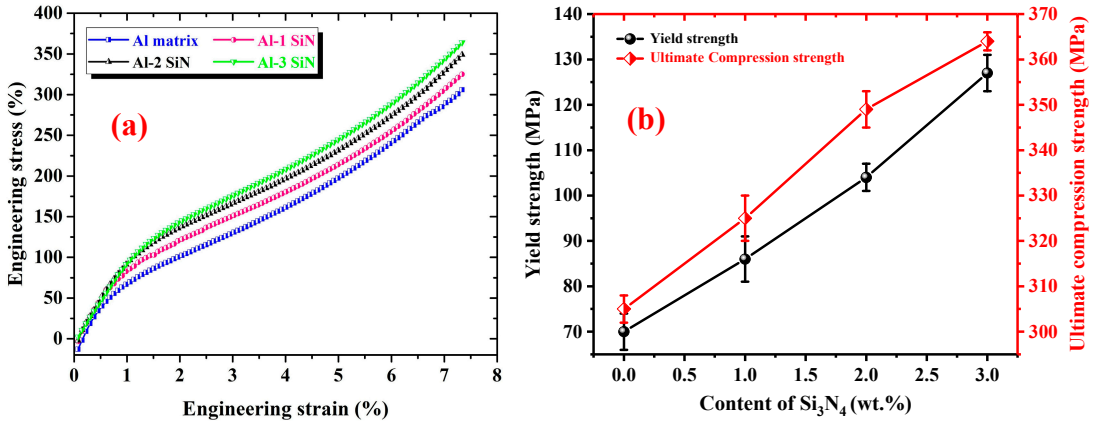

Figure 6. (**a**) The compression stress-strain curves and (**b**) mechanical data of Al-Si_3N_4 nanocomposites.

It can be seen that the yield strength (YS) and ultimate compressive strength (UCS) significantly increase with the addition of amorphous Si_3N_4 content. The value of yield strength (YS) obtained for Al-3wt.% Si_3N_4 composite was 127 ± 4 MPa, with an ultimate compressive strength (UCS) of 364 ± 2 MPa at a uniform failure strain of 7.4%. The increase in yield strength and compressive strength of the nanocomposites can be attributed to the strengthening mechanisms because of the effective load transfer between the matrix and reinforcement particles, dispersion hardening effect and uniform distribution of reinforcement particles in the matrix [31,32].

Table 1. Microhardness, yield strength and ultimate compressive strength of Al-Si_3N_4 nanocomposites.

Composition	Microhardness (Hv)	CYS (MPa)	UCS (MPa)	Failure Strain (%)
Pure Al	38 ± 3	70 ± 4	305 ± 3	>7
Al-1wt.% Si_3N_4	43 ± 5	86 ± 5	325 ± 5	>7
Al-2wt.% Si_3N_4	58 ± 3	104 ± 3	349 ± 4	>7
Al-3wt.% Si_3N_4	77 ± 2	127 ± 4	364 ± 2	>7
Al-3wt.% Si_3N_4 [29]	57 ± 2	198 ± 21	292 ± 18	–
Al-9wt.% Si_3N_4 [33]	59.5	–	–	–
Al alloy-3wt.% Si_3N_4 [34]	82	—	—	–

There are several strengthening mechanisms and theories to enhance the mechanical properties of the composite materials. In the present study, the main strengthening mechanism is dispersion hardening. Dispersion hardening, also known as Orowan strengthening, is caused by the dispersed second phase. The Orowan strengthening mechanism is given by the Orowan-Ashby equation [35].

$$\sigma_{Orowan} = \frac{0.13Gb}{\lambda} \ln \frac{d}{2b} \quad (1)$$

where G is the shear modulus of Al, b is the Burgers vector of Al, d is the average diameter of nanoparticles, and λ is the interparticulate distance between the reinforcement particles, which is given by the following equation [36].

$$\lambda = d\left[\left(\frac{1}{2f}\right)^{1/3} - 1\right] \quad (2)$$

where, f is the volume fraction of the reinforcement particles.

3.6. Fractography of Al-Si_3N_4 Nanocomposites

The fracture morphology analysis of the microwave sintered pure Al and Al-Si_3N_4 nanocomposites tested under compression loading is shown in Figure 7. A typical shear mode fracture can be observed in the nanocomposites and the fracture surfaces show the cracks at 45° to the compression loading axis. The compressive deformations obtained in Al composites are indifferent. This is due to the work hardening behavior. The plastic deformations of the composites are restricted by the presence of a dispersion of the second phase in the matrix [37].

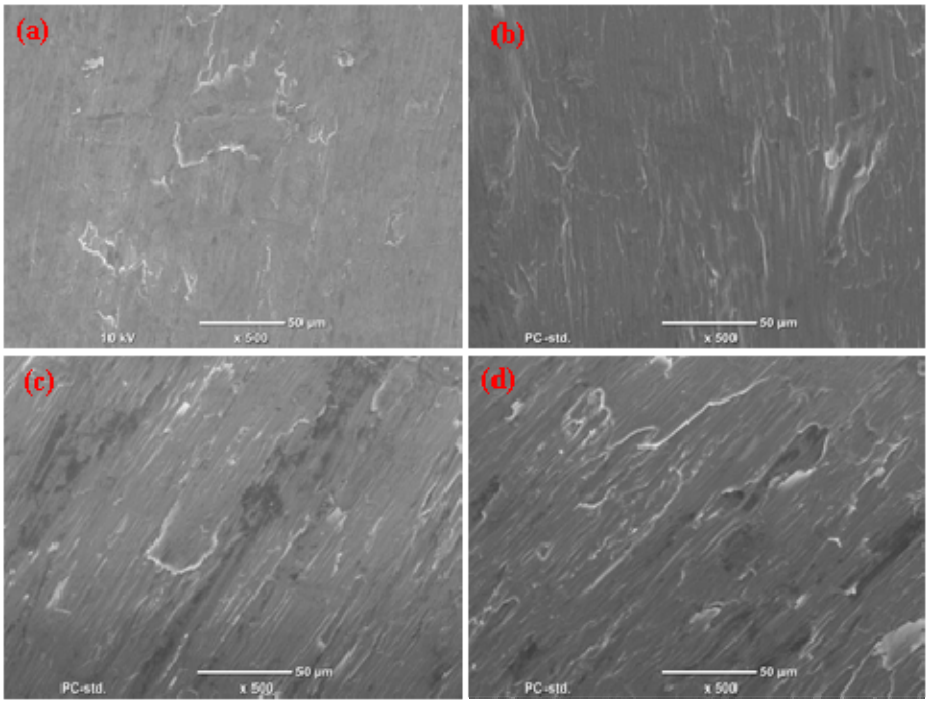

Figure 7. (**a**–**d**) Compression fracture surface images of Al-Si_3N_4 nanocomposites.

4. Conclusions

In this study, amorphous Si_3N_4 nanoparticle reinforced Al matrix nanocomposites were successfully synthesized using microwave sintering process. The effect of amorphous Si_3N_4 content on the microstructural and mechanical of the developed Al composites are investigated. Experimental density of the synthesized composites increased with the increase in amorphous Si_3N_4 content, while porosity slightly decreased. The XRD analysis reveals the presence of amorphous Si_3N_4 in Al matrix. SEM and EDX analyses show the uniform distribution of amorphous Si_3N_4 nanoparticles in the aluminum matrix. Hardness, Yield strength and compressive strengths of the nanocomposites increased with an increasing silicon nitride content, hence, Al-3wt.%Si_3N_4 nanocomposite exhibited enhanced hardness (77 $\pm$ 2 Hv), yield strength (27 $\pm$ 4 MPa) and UCS (364 $\pm$ 2 MPa).

Author Contributions: A.S. and A.M.A.M. proposed the original project and supervised the investigation. M.R.M. and P.R.M. performed the experiments, analyzed the data, and wrote the paper with assistance from all authors. All authors contributed to the discussions in the manuscript.

Funding: This publication was made possible by NPRP Grant 7-159-2-076 from the Qatar National Research Fund (a member of the Qatar Foundation). Statements made herein are solely the responsibility of the authors.

Conflicts of Interest: The authors declare no conflict of interest.

References

1. Zweben, C. Composite Materials. In *Mechanical Engineers*, 4th ed.; John Wiley & Sons, Inc.: Hoboken, NJ, USA, 2015; pp. 1–37.
2. Guild, F.J.; Taylor, A.C.; Downes, J. Composite Materials. In *Encyclopedia of Maritime and Offshore Engineering*, 1st ed.; John Wiley & Sons, Inc.: Hoboken, NJ, USA, 2017.
3. Li, J.; Gao, W. Oxidation of Metal Matrix Composites. In *Developments in High-Temperature Corrosion and Protection of Materials*; Woodhead Publishing: Cambridge, UK, 2008; pp. 365–397.
4. Hunt, W.H. Metal matrix composites. *Compr. Comp. Mater.* **2000**, *6*, 57–66.
5. Miracle, D.B. Metal matrix composites-from science to technological significance. *Compos. Sci. Technol.* **2005**, *65*, 2526–2540. [CrossRef]
6. Alan, R.B. Applications for metal matrix composites. *Metal Pow. Rep.* **1991**, *46*, 42–45.
7. Rohit, S.; Saurabh, J.P.; Khushboo, K.; Kushal, K.; Pardeep, S. A review of the aluminium metal matrix composite and its properties. *Inter. Res. J. Eng. Tech.* **2017**, *4*, 832–842.
8. Prasad, S.V.; Asthana, R. Aluminum metal-matrix composites for automotive applications: Tribological considerations. *Tribol. Lett.* **2004**, *17*, 445–453. [CrossRef]
9. Kanthavel, K.; Sumesh, K.R.; Saravanakumar, P. Study of tribological properties on $Al/Al_2O_3/MoS_2$ hybrid composite processed by powder metallurgy. *Alex. Eng. J.* **2016**, *55*, 13–17. [CrossRef]
10. Shivananda Murthy, K.V.; Girish, D.P.; Keshavamurthy, R.; Temel, V.; Praveennath, G.K. Mechanical and thermal properties of $AA7075/TiO_2$/Fly ash hybrid composites obtained by hot forging. *Prog. Nat. Sci. Mater. Int.* **2017**, *27*, 474–481. [CrossRef]
11. Sambathkumar, M.; Navaneethakrishnan, P.; Ponappa, K.; Sasikumar, K.S.K. Mechanical and corrosion behavior of Al7075 (hybrid) metal matrix composites by two step stir casting process. *Latin Am. J. Solid Struct.* **2017**, *14*, 243–255. [CrossRef]
12. Reddy, M.P.; Ubaid, F.; Shakoor, R.A.; Gururaj, P.; Vyasaraj, M.; Mohamed, A.M.A.; Gupta, M. Effect of reinforcement concentration on the properties of hot extruded Al-Al2O3 composites synthesized through microwave sintering process. *Mater. Sci. Eng. A* **2017**, *696*, 60–69. [CrossRef]
13. Fei, T.; Anderson, I.E.; Gnaupel-Herold, T.; Prask, H. Pure Al matrix composites produced by vacuum hot pressing: Tensile properties and strengthening mechanisms. *Mater. Sci. Eng. A* **2004**, *383*, 362–373.
14. Ghasali, E.; Pakseresht, A.H.; Rahbari, A.E.; Hossein, A.; Masoud, E.; Ebadzadeh, T. Mechanical properties and microstructure characterization of spark plasma and conventional sintering of Al-SiC-TiC composites. *J. Alloys Compd.* **2016**, *666*, 366–371. [CrossRef]
15. Madhusudan, S.; Sarcar, M.M.M.; Rao, N.B.R.M. Mechanical properties of Aluminum-Copper(p) composite metallic materials. *J. Appl. Res. Tech.* **2016**, *14*, 293–299. [CrossRef]
16. Flom, Y.; Arsenault, R.J. Effect of particle size on fracture toughness of SiC/Al composite material. *Acta Metal.* **1989**, *37*, 2413–2423. [CrossRef]
17. Aghajanian, M.K.; Macmillan, N.H.; Kennedy, C.R.; Luszcz, S.J.; Roy, R. Properties and microstructures of Lanxide Al_2O_3-Al ceramic composite materials. *J. Mater. Sci.* **1989**, *24*, 658–670. [CrossRef]
18. Moradi, M.R.; Moloodi, A.; Habibolahzadeh, A. Fabrication of nano-composite Al-B_4C foam via powder metallurgy-space holder technique. *Pro. Mater. Sci.* **2015**, *11*, 553–559. [CrossRef]
19. Chenxu, Z.; Dongxu, Y.; Jinwei, Y.; Kaihui, Z.; Yongfeng, X.; Hanqin, L.; Yu, P.Z. Microstructure and mechanical properties of aluminum matrix composites reinforced with pre-oxidized β-Si3N4 whiskers. *Mater. Sci. Eng. A* **2018**, *723*, 109–117.
20. Chung, Y.K.; Koo, J.H.; Kim, S.A.; Chi, E.O.; Cho, J.Y.; Sohn, W.B.; Kim, M.Y.; Park, C. Growth mechanism of Si_3N_4 nanowires from amorphous Si_3N_4 powders synthesized by low-temperature vapor-phase reaction. *Cryst. Eng. Comm.* **2016**, *18*, 3247–3255. [CrossRef]
21. Wang, Q.; Hou, J.; Zhu, H. Synthesis and characterization of amorphous silicon nitride nanoparticles and α-silicon nitride nanowires. In *TMS 2015 144th Annual Meeting & Exhibition*; Springer: Cham, Switzerland, 2015; pp. 317–323.
22. Reddy, M.P.; Shakoor, R.A.; Parande, G.; Manakari, V.; Ubaid, F.; Mohamed, A.M.A.; Gupta, M. Enhanced performance of nano-sized SiC reinforced Al metal matrix nanocomposites synthesized through microwave sintering and hot extrusion techniques. *Prog. Nat. Sci. Mater.* **2017**, *27*, 607–615. [CrossRef]

23. Dipti, K.D.; Purna, C.M.; Saranjit, S.; Ratish, K.T. Properties of ceramic-reinforced aluminum matrix composites-a review. *Int. J. Mech. Mater. Eng.* **2014**, *9*. [CrossRef]
24. Vamsi Krishna, M.; Anthony, X.M. Experiment and statistical analysis of end milling parameters for Al/SiC using response surface methodology. *Int. J. Eng. Tech.* **2015**, *7*, 2274–2285.
25. Dou, Y.C.; Qin, X.Y.; Li, D.; Li, Y.Y.; Xin, H.X.; Zhang, J.; Liu, Y.F.; Song, C.J.; Wang, L. Enhanced thermoelectric performance of BiSbTe-based composites incorporated with amorphous Si_3N_4 nanoparticles. *RSC Adv.* **2015**, *5*, 34251–34256. [CrossRef]
26. Reddy, M.P.; Ubaid, F.; Shakoor, R.A.; Gururaj, P.; Vyasaraj, M.; Yousuf, M.; Mohamed, A.M.A.; Gupta, M. Improved properties of Al-Si_3N_4 nanocomposites fabricated through a microwave sintering and hot extrusion process. *RSC Adv.* **2017**, *7*, 34401–34410.
27. Ubaid, F.; Reddy, M.P.; Shakoor, R.A.; Gururaj, P.; Vyasaraj, M.; Mohamed, A.M.A.; Gupta, M. Using B4C nanoparticles to enhance thermal and mechanical response of aluminum. *Materials* **2017**, *10*, 621. [CrossRef] [PubMed]
28. Reddy, M.P.; Vyasaraj, M.; Gururaj, P.; Shakoor, R.A.; Mohamed, A.M.A.; Gupta, M. Enhancing compressive, tensile, thermal and damping response of pure Al using BN nanoparticles. *J. Alloys Compd.* **2018**, *762*, 398–408. [CrossRef]
29. Mahmut, C.S.; Gürbüz, M.; Koç, E. Fabrication and characterization of SiC and Si_3N_4 reinforced aluminum matrix composites. *Uni. J. Mater. Sci.* **2017**, *5*, 95–101.
30. Liu, G.R. A step-by-step method of rule-of-mixture of fiber- and particle-reinforced composite materials. *Compos. Struct.* **1997**, *40*, 313–322. [CrossRef]
31. Miller, W.S.; Humphreys, F.J. Strengthening mechanisms in particulate metal matrix composites. *Scr. Metal. Mater.* **1991**, *25*, 33–38. [CrossRef]
32. Morteza, A. Strengthening mechanisms in particulate Al/B4C composites produced by repeated roll bonding process. *J. Alloys Compd.* **2011**, *509*, 2243–2247.
33. Ankit, T.; Sharma, D. Characterization of AA6082/Si3N4 composites. In Proceedings of the 21st International Conference on New Frontiers in Engineering, Science & Technology, New Delhi, India, 8–12 January 2018.
34. Pardeep, S.; Satpal, S.; Dinesh, K. Production and some properties of Si_3N_4 reinforced aluminium alloy composites. *J. Asian Ceram. Soc.* **2015**, *3*, 352–359.
35. Dieter, G.E.; Bacon, D. *Mechanical Metallurgy*; McGraw-Hill: New York, NY, USA, 1986.
36. Ramezanalizadeh, H.; Emamy, M.; Shokouhimehr, M. A novel aluminum based nanocomposite with high strength and good ductility. *J. Alloys Compd.* **2015**, *649*, 461–473. [CrossRef]
37. Reddy, M.P.; Ubaid, F.; Shakoor, R.A.; Mohamed, A.M.A. Comparative study of structural and mechanical properties of Al-Cu composites prepared by vacuum and microwave sintering techniques. *J. Mater. Res. Tech.* **2017**, *7*, 165–172.